Results in Chemistry 19 (2026) 102907

Contents lists available at ScienceDirect

Results in Chemistry

journal homepage: www.sciencedirect.com/journal/results-in-chemistry

Development of new piperazine tethered pyridine derivatives as inhibitors of BAD phosphorylation in human breast cancer

Dileep Nagaraju [a], Pushpa H. Chandraiah [b], Bhoomika B. Ravi [a], Sindhu M. Parameshwaraiah [a], Mamatha S. Kempasiddegowda [c], Toreshettahally R. Swaroop [a], Santosh L. Goankar [d], Kanchugarakoppal S. Rangappa [e,*], Basappa Basappa [a,*]

[a] Department of Studies in Organic Chemistry, University of Mysore, Manasagangotri, Mysuru 570006, Karnataka, India
[b] Strides Pharma Science Limited, Bilekahalli, Bannerghatta Road, Bengaluru 560076, Karnataka, India
[c] Tsinghua-Berkeley Shenzhen Institute and The Institute of Biopharmaceutical and Health Engineering, Tsinghua Shenzhen International Graduate School, Tsinghua University, Shenzhen 518055, People's Republic of China
[d] Department of Chemistry, Manipal Institute of Technology, Manipal Academy of Higher Education, Manipal 576104, Karnataka, India
[e] Institution of Excellence, University of Mysore, Manasagangotri, Mysuru 570 006, Karnataka, India

ARTICLE INFO

Keywords:
Pyridine
Piperazine
Breast cancer
Cytotoxic

ABSTRACT

Breast cancer is a devastating disease responsible for many deaths worldwide. Although many drugs are available for its treatment, new anticancer agents are demand due to undesirable side effects of well accepted drugs. Many anticancer drugs contain piperazine and pyridine moieties. We previously discovered piperazine containing small molecule called NPB [*N*-cyclopentyl-3-((4-(2,3-dichlorophenyl)piperazin-1-yl)(2-hydroxyphenyl)methyl)benzamide] that targeted pBAD (BCL-2-associated death) in human breast cancer cells. Inspired by these molecules, we have designed new piperazine tethered pyridine compounds. The synthesized compounds were evaluated for their cytotoxic activity against MCF-7 breast cancer cells. A compound, *N*-(3-(6-chloro-5-methylpyridin-3-yl) phenyl)-2-(4-(2-nitrophenyl)piperazin-1-yl)acetamide (**7h**) showed the highest cytotoxic activity (6.15 μM) against MCF-7. A fair structure activity relationship has been discussed. The molecular modeling studies indicated that our title compounds induced cancer cell death *via* inhibition of phosphorylation of BCL-2-associated death (BAD) promoter. The results of these studies are presented in this article.

1. Introduction

Among different types of cancer, breast cancer is responsible for 0.67 million deaths worldwide, which makes it the second most common cancer overall. According to the World Health Organization (WHO), 2.3 million new cases were diagnosed in 2022. Recently, it has surpassed lung cancer. Although it can be treatable, it remains the most common cause of death, in particular, low-income countries. The WHO has been trying to reduce the mortality rates by 2.5 % annually through its initiatives. Early detection and awareness about breast cancer could enhance survival rates.

Piperazine is a most privileged scaffold in medicinal chemistry with diverse biological activities [1]. The two nitrogen atoms present in it enhance polar surface area, rigidity, tendency of hydrogen bonding, water solubility, bioavailability, affinity and specificity. Further, piperazine derivatives are potent anticancer agents [2]. Many well-accepted anticancer drugs contain piperazine moiety. They are Abemaciclib, Bosutinib, Brigatinib, Dasatinib, Imatinib, Palbociclib, Ponatinib, Venetoclax and Olaparib.

On the other hand, pyridine has its own significance in medicinal chemistry due to many pharmacological properties [3,4]. Notably, pyridine also shows potential anticancer properties [5]. Some FDA approved anticancer drugs such as Crizotinib, Vismodegib, Regorafenib and Sorafenib contain pyridine nucleus.

Further, phosphorylation BCL-2-associated death promoter (pBAD) is essential for survivability of cancer cells [6,7]. This survivability is possible when BCL-2-associated death (BAD) promoter is phosphorylated at Ser-75, Ser-99, and Ser-118 [8]. Many pathways such as RAS/RAF/MAPK and PI3K/AKT/mTOR are responsible for BAD phosphorylation [9]. Thus, phosphorylated BAD is the critical reason for the development of cancer, its progression and therapeutic resistance [9]. Therefore, inhibition of BAD phosphorylation is a key strategy to treat

* Corresponding authors.
E-mail addresses: rangappaks@gmail.com (K.S. Rangappa), salundibasappa@gmail.com (B. Basappa).

https://doi.org/10.1016/j.rechem.2025.102907
Received 15 August 2025; Accepted 21 November 2025
Available online 22 November 2025

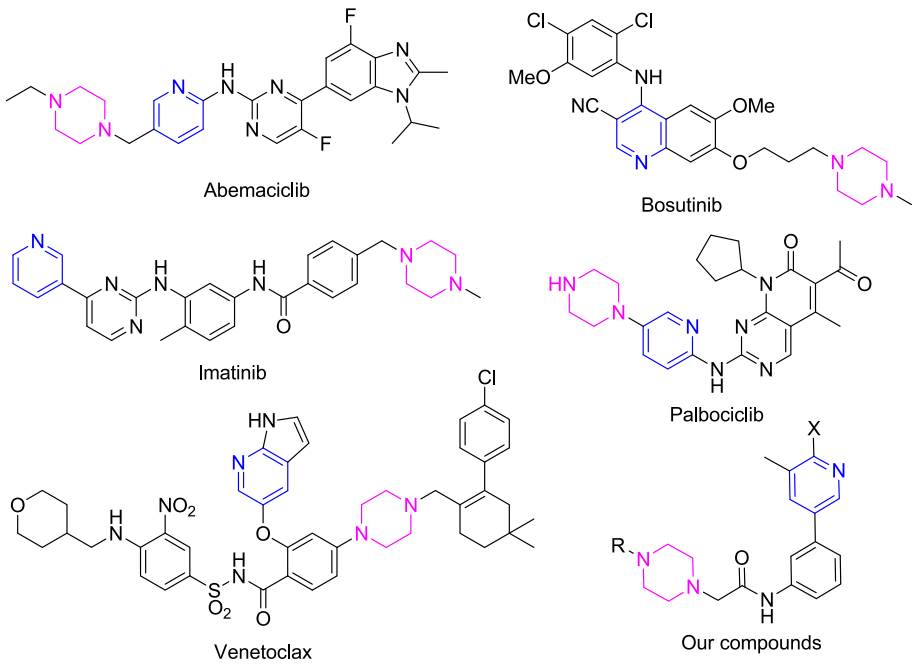

Fig. 1. Anticancer drugs and our compounds containing piperazine and pyridine moieties.

cancer.

Notably, some commercially available anticancer drugs containing both piperazine and pyridine moieties are presented in Fig. 1. Inspired by these drugs, we have designed new piperazine and pyridine containing molecules, which are analogues to NPB [*N*-cyclopentyl-3-((4-(2,3-dichlorophenyl)piperazin-1-yl)(2-hydroxyphenyl)methyl)benzamide]. It should be noted that, this NPB is a well-known inhibitor of BAD phosphorylation at Ser-99 [10,11].

We are active in organic synthesis [12–14] and anticancer research [10,11,15–17]. Our efforts in this direction has motivated us to develop new piperazine tethered pyridine derivatives and evaluation of their anticancer effects on MCF-7 cell lines. The possible mode of action of these compounds has been predicted with the help of molecular modeling. The results of these studies are presented in this article.

2. Experimental

2.1. Materials and methods

All chemicals, reagents and solvents were purchased from commercial suppliers in India and were used without further purification. All reactions were monitored by thin layer chromatographic technique (commercially available precoated plates, MERCK 60F254, 0.25 mm thickness) and were visualized using UV light. Melting points were recorded by Superfit India melting apparatus and are uncorrected. IR spectra were recorded using PerkinElmer spectrometer. NMR spectra were recorded using Bruker NMR spectrometer. Chemical shifts (δ) are given in ppm relative to residual solvent peak. DMSO-d_6 was used as a solvent and tetramethylsilane was used as internal standard. Coupling constant (J) values are specified in Hz. Mass spectra were recorded by using a Waters-SynaptG2 mass spectrometer. Procell Life Science and Technology Co., Ltd. (Wuhan, China) was the supplier of MCF-7, which was cultivated in accordance with ATCC propagation guidelines.

2.2. Procedures

2.2.1. Procedure for the synthesis of 3-(6-fluoro/chloro-5-methylpyridin-3-yl)aniline (3)

To a solution of 3-bromoaniline **1** (1 mmol) in aqueous THF (H_2O: THF::4:1, 5 mL), potassium carbonate (3 mmol), (6-halo-5-methylpyridin-3-yl)boronic acid **2** (1 mmol) and Pd(dppf)Cl_2 (0.1 mmol) were added in a 100 mL pressure seal tube. The contents were stirred for 4–5 h at 80 °C. The progress of the reaction was analyzed by TLC. After its completion, water (25 mL) was added and extracted with ethyl acetate (25 mL × 2). Products **3** were purified by column chromatography with silica gel (60–120 mesh) as stationary phase and a mixture of ethyl acetate in hexane (2:8) as eluent.

2.2.2. Procedure for the synthesis of 2-chloro-N-(3-(6-fluoro/chloro-5-methylpyridin-3-yl)phenyl)acetamide (5)

To a solution of **3** (1 mmol) in THF (3 mL), chloroacetyl chloride **4** (1 mmol) was added followed by the addition of triethylamine (1 mmol) at 0 °C. The reaction mixture was stirred for 4 h. After the completion of reaction (monitored by TLC), water 25 mL was added. A solid separated, was filtered using Buchner funnel and dried.

2.2.3. Procedure for the synthesis of piperazine tethered pyridine derivatives (7a-k)

To a solution of **5** (1 mmol) in acetone (5 mL), 1-arylpiperazines **6** (1 mmol) and triethylamine (1 mmol) were added. The contents were refluxed for 4–5 h. After the completion of reaction (monitored by TLC), acetone was removed under reduced pressure. The residue was suspended in brine (25 mL) and extracted with ethyl acetate (25 mL × 2). The combined organic layer was dehydrated over anhydrous Na_2SO_4 and concentrated. The so obtained crude products were purified by column chromatography with silica gel (60–120 mesh) as stationary phase and a mixture of ethyl acetate in hexane (3:7) as mobile phase.

2.2.4. Alamar blue assay

The cytotoxicity of title compounds **7a-k** were analyzed against MCF-7 cells following Alamar Blue assay [18–20]. Briefly, compounds were dissolved in DMSO such that concentrations of the resulting solutions were 10 mg/mL and they were preserved at −20 °C. The solutions were diluted again before treating with culture media. A total of 2×10^3 cells/well was plated in 96-well plates. After 6 h, the cells were treated with varying concentrations of title compounds in triplicates. Reagent (20 μL of concentration 5 mg/mL) was added to the cells during the last 4 h of their time point for 72 h as per manufacturer's instructions. The

media were removed from the wells after 4 h of reagent addition. Finally, the absorbances were measured at 590 nm in an enzyme-linked immunosorbent assay reader.

2.3. Spectral data

2.3.1. 2-(4-(2,3-Dichlorophenyl)piperazin-1-yl)-N-(3-(6-fluoro-5-methylpyridin-3-yl)phenyl)acetamide (7a)

Yellowish orange solid; m.p. 144–146 °C; IR (neat): 3305, 2941, 1675, 1595, 1340, 869 cm^{-1}; ^1H NMR (400 MHz, DMSO-d_6) δ 9.93 (s, 1H, N—H), 8.34 (s, 1H, Ar—H), 8.14 (d, J = 8.0 Hz, 1H, Ar—H), 8.00 (s, 1H, Ar—H), 7.79 (d, J = 8.0 Hz, 1H, Ar—H), 7.43–7.51 (m, 2H, Ar—H), 7.34–7.37 (m, 2H, Ar—H), 7.22 (d, J = 8.0 Hz, 1H, Ar—H), 3.30 (s, 2H, CH_2), 3.04–3.19 (m, 4H, $(CH_2)_2$), 2.74–2.85 (m, 4H, $(CH_2)_2$), 2.37 (s, 3H, CH_3); ^{13}C NMR (100 MHz, DMSO-d_6) δ 168.9, 161.7 (d, J = 234.0 Hz), 151.6, 142.8 (d, J = 15.0 Hz), 141.0, 139.8, 137.0, 134.7, 133.1, 130.0, 128.9, 126.5, 124.9, 122.4, 120.1, 120.0, 119.6, 118.3, 62.1, 53.3, 51.3, 14.5; HRMS (ESI): m/z $[M + H]^+$ calcd for $C_{24}H_{23}Cl_2FN_4O$: 473.1311; found: 473.1313.

2.3.2. 2-(4-(4-Chlorophenyl)piperazin-1-yl)-N-(3-(6-fluoro-5-methylpyridin-3-yl)phenyl)acetamide (7b)

White solid; m.p. 138–140 °C; IR (neat): 3304, 2940, 1677, 1594, 1360, 969 cm^{-1}; ^1H NMR (400 MHz, DMSO-d_6) δ 9.91 (s, 1H, N—H), 8.32 (s, 1H, Ar—H), 8.12 (d, J = 8.0 Hz, 1H, Ar—H), 7.98 (s, 1H, Ar—H), 7.78 (d, J = 8.0 Hz, 1H, Ar—H), 7.41–7.49 (m, 2H, Ar—H), 7.26 (d, J = 8.0 Hz, 2H, Ar—H), 6.99 (d, J = 8.0 Hz, 2H, Ar—H), 3.20–3.31 (m, 6H, CH_2 & $(CH_2)_2$), 2.71–2.77 (m, 4H, $(CH_2)_2$), 2.35 (s, 3H, CH_3); ^{13}C NMR (100 MHz, DMSO-d_6) δ 168.9, 161.7 (d, J = 234.0 Hz), 150.3, 142.8 (d, J = 15.0 Hz), 140.9 (d, J = 6.0 Hz), 139.7, 137.0, 130.0, 129.1, 122.8, 122.4, 120.0, 119.6, 119.5, 118.3, 117.3, 62.1, 53.0, 48.3, 14.5; HRMS (ESI): m/z $[M + H]^+$ calcd for $C_{24}H_{24}ClFN_4O$: 439.1701; found: 439.1700.

2.3.3. N-(3-(6-Fluoro-5-methylpyridin-3-yl)phenyl)-2-(4-(2-nitrophenyl) piperazin-1-yl)acetamide (7c)

Yellowish orange liquid; IR (neat): 3302, 2942, 1679, 1598, 1365, 971 cm^{-1}; ^1H NMR (400 MHz, DMSO-d_6) δ 9.94 (s, 1H, N—H), 8.35 (s, 1H, Ar—H), 8.14 (d, J = 8.0 Hz, 1H, Ar—H), 8.00 (s, 1H, Ar—H), 7.78–7.86 (m, 2H, Ar—H), 7.64 (t, J = 8.0 Hz, 1H, Ar—H), 7.39–7.51 (m, 3H, Ar—H), 7.18 (t, J = 8.0 Hz, 1H, Ar—H), 3.29 (s, 2H, CH_2), 3.09–3.19 (m, 4H, $(CH_2)_2$), 2.70–2.79 (m, 4H, $(CH_2)_2$), 2.37 (s, 3H, CH_3); ^{13}C NMR (100 MHz, DMSO-d_6) δ 168.9, 161.7 (d, J = 234.0 Hz), 145.7, 143.3, 142.8 (d, J = 15.0 Hz), 141.0 (d, J = 7.0 Hz), 139.7, 137.0, 134.7, 134.3, 130.0, 125.9, 122.4, 122.3, 121.9, 120.0, 119.6, 118.3, 62.0, 53.1, 51.5, 14.5; HRMS (ESI): m/z $[M + H]^+$ calcd for $C_{24}H_{24}FN_5O_3$: 450.1941; found: 450.1944.

2.3.4. 2-(4-(4-Chloro-2-fluorophenyl)piperazin-1-yl)-N-(3-(6-fluoro-5-methylpyridin-3-yl)phenyl)acetamide (7d)

White solid; m.p. 144–146 °C; IR (neat): 3300, 2938, 1674, 1599, 1368, 975 cm^{-1}; ^1H NMR (400 MHz, DMSO-d_6) δ 9.98 (s, 1H, N—H), 8.33 (s, 1H, Ar—H), 8.12 (d, J = 12.0 Hz, 1H, Ar—H), 7.99 (s, 1H, Ar—H), 7.78 (d, J = 8.0 Hz, 1H, Ar—H), 7.35–7.50 (m, 3H, Ar—H), 7.21–7.24 (m, 1H, Ar—H), 7.10 (t, J = 8.0 Hz, 1H, Ar—H), 3.32 (s, 2H, CH_2), 3.09–3.20 (m, 4H, $(CH_2)_2$), 2.78–2.86 (m, 4H, $(CH_2)_2$), 2.36 (s, 3H, CH_3); ^{13}C NMR (100 MHz, DMSO-d_6) δ 170.4, 165.8 (d, J = 579.0 Hz), 158.4 (d, J = 425.0 Hz), 153.8, 142.7 (d, J = 15.0 Hz), 140.9 (d, J = 6.0 Hz), 139.7, 139.4 (d, J = 8.0 Hz), 137.0, 134.7 (d, J = 4.0 Hz), 130.0, 125.7 (d, J = 10.0 Hz), 125.2, 121.6 (d, J = 161.0 Hz), 119.8 (d, J = 33.0 Hz), 118.9 (d, J = 128.0 Hz), 117.1, 116.8, 61.9, 52.3, 50.2, 14.5; HRMS (ESI): m/z $[M + H]^+$ calcd for $C_{24}H_{23}ClF_2N_4O$: 457.1607; found: 457.1605.

2.3.5. N-(3-(6-Fluoro-5-methylpyridin-3-yl)phenyl)-2-(4-(p-tolyl) piperazin-1-yl)acetamide (7e)

White solid; m.p. 142–144 °C; 3294, 2835, 1677, 1594, 1388, 806; ^1H NMR (400 MHz, DMSO-d_6) δ 9.90 (s, 1H, N—H), 8.29 (s, 1H, Ar—H), 8.09 (d, J = 8.0 Hz, 1H, Ar—H), 7.95 (s, 1H, Ar—H), 7.75 (d, J = 8.0 Hz, 1H, Ar—H), 7.38–7.46 (m, 2H, Ar—H), 7.03 (d, J = 8.0 Hz, 2H, Ar—H), 6.85 (d, J = 8.0 Hz, 2H, Ar—H), 3.22 (s, 2H, CH_2), 3.11–3.17 (m, 4H, $(CH_2)_2$), 2.71–2.77 (m, 4H, $(CH_2)_2$), 2.32 (s, 3H, CH_3), 2.20 (s, 3H, CH_3); ^{13}C NMR (100 MHz, DMSO-d_6) δ 170.4, 168.8, 161.7 (d, J = 234.0 Hz), 149.4, 142.8 (d, J = 15.0 Hz), 140.9, 137.0, 134.6, 130.0, 129.8, 128.1, 122.4, 120.0, 119.6, 118.3, 116.2, 53.2, 52.5, 48.9, 20.5, 14.5; HRMS (ESI): m/z $[M + H]^+$ calcd for $C_{25}H_{27}FN_4O$: 419.2247; found: 419.2248.

2.3.6. N-(3-(6-Fluoro-5-methylpyridin-3-yl)phenyl)-2-(4-(2-fluorophenyl) piperazin-1-yl)acetamide (7f)

Brown solid; m.p. 142–144 °C; IR (neat): 3306, 2940, 1676, 1600, 1364, 978 cm^{-1}; ^1H NMR (400 MHz, DMSO-d_6) δ 9.92 (s, 1H, N—H), 8.33 (s, 1H, Ar—H), 8.11 (d, J = 8.0 Hz, 1H, Ar—H), 8.00 (s, 1H, Ar—H), 7.79 (d, J = 8.0 Hz, 1H, Ar—H), 7.41–7.49 (m, 2H, Ar—H), 7.08–7.18 (m, 4H, Ar—H), 3.28 (s, 2H, CH_2), 3.14–3.20 (m, 4H, $(CH_2)_2$), 2.75–2.84 (m, 4H, $(CH_2)_2$), 2.35 (s, 3H, CH_3); ^{13}C NMR (100 MHz, DMSO-d_6) δ 170.4, 168.9, 162.9, 161.4, 160.6, 155.4 (d, J = 243.0 Hz), 142.8 (d, J = 15.0 Hz), 141.0, 140.3, 139.8, 137.0, 134.7, 130.0, 125.3, 122.4, 119.7, 118.3, 116.4 (d, J = 20.0 Hz), 53.8, 52.5, 50.4, 14.5; HRMS (ESI): m/z $[M + H]^+$ calcd for $C_{24}H_{24}F_2N_4O$: 423.1996; found: 423.1994.

2.3.7. N-(3-(6-Chloro-5-methylpyridin-3-yl)phenyl)-2-(4-(2,3-dichlorophenyl)piperazin-1-yl)acetamide (7 g)

Orange solid; m.p. 144–146 °C; IR (neat): 3301, 2942, 1679, 1602, 1361, 981 cm^{-1}; ^1H NMR (400 MHz, DMSO-d_6) δ 9.89 (s, 1H, N—H), 8.51 (s, 1H, Ar—H), 7.98–8.06 (m, 2H, Ar—H), 7.77 (d, J = 8.0 Hz, 1H, Ar—H), 7.40–7.47 (m, 2H, Ar—H), 7.30–7.34 (m, 2H, Ar—H), 7.16 (d, J = 4.0 Hz, 1H, Ar—H), 3.25 (s, 2H, CH_2), 2.99–3.15 (m, 4H, $(CH_2)_2$), 2.69–2.80 (m, 4H, $(CH_2)_2$), 2.41 (s, 3H, CH_3); ^{13}C NMR (100 MHz, DMSO-d_6) δ 169.0, 151.6, 150.1, 145.3, 139.8, 138.5, 136.8, 135.6, 133.1, 132.7, 130.1, 128.9, 126.5, 124.9, 122.5, 120.1, 119.1, 118.3, 62.1, 53.3, 51.3, 19.5; HRMS (ESI): m/z $[M + H]^+$ calcd for $C_{24}H_{23}Cl_3N_4O$: 489.1016; found: 489.1014.

2.3.8. N-(3-(6-Chloro-5-methylpyridin-3-yl)phenyl)-2-(4-(2-nitrophenyl) piperazin-1-yl)acetamide (7 h)

Red viscous liquid; IR (neat): 3308, 2940, 1676, 1594, 1366, 975 cm^{-1}; ^1H NMR (400 MHz, DMSO-d_6) δ 9.95 (s, 1H, N—H), 8.57 (s, 1H, Ar—H), 8.12 (s, 1H, Ar—H), 8.02 (s, 1H, Ar—H), 7.81–7.87 (m, 2H, Ar—H), 7.65 (t, J = 8.0 Hz, 1H, Ar—H), 7.46–7.53 (m, 2H, Ar—H), 7.40 (d, J = 8.0 Hz, 1H, Ar—H), 7.18 (t, J = 8.0 Hz, 1H, Ar—H), 3.29 (s, 2H, CH_2), 3.09–3.19 (m, 4H, $(CH_2)_2$), 2.67–2.78 (m, 4H, $(CH_2)_2$), 2.47 (s, 3H, CH_3); ^{13}C NMR (100 MHz, DMSO-d_6) δ 172.5, 168.9, 150.1, 145.7, 145.3, 143.4, 139.8, 138.5, 136.7, 135.6, 134.2, 132.7, 130.1, 125.9, 122.5, 121.9, 119.9, 118.3, 62.0, 53.1, 51.5, 19.5; HRMS (ESI): m/z $[M + H]^+$ calcd for $C_{24}H_{24}ClN_5O_3$: 466.1646; found: 466.1645.

2.3.9. N-(3-(6-Chloro-5-methylpyridin-3-yl)phenyl)-2-(4-(p-tolyl) piperazin-1-yl)acetamide (7i)

Pale yellow solid; m.p. 154–156 °C; IR (neat): 3304, 2935, 1679, 1597, 1368, 971 cm^{-1}; ^1H NMR (400 MHz, DMSO-d_6) δ 9.87 (s, 1H, N—H), 8.51 (s, 1H, Ar—H), 8.07 (s, 1H, Ar—H), 7.97 (s, 1H, Ar—H), 7.77 (d, J = 8.0 Hz, 1H, Ar—H), 7.41–7.47 (m, 2H, Ar—H), 7.02 (d, J = 8.0 Hz, 2H, Ar—H), 6.85 (d, J = 8.0 Hz, 2H, Ar—H), 3.22 (s, 2H, CH_2), 3.15–3.17 (m, 4H, $(CH_2)_2$), 2.66–2.69 (m, 4H, $(CH_2)_2$), 2.41 (s, 3H, CH_3), 2.20 (s, 3H, CH_3); ^{13}C NMR (100 MHz, DMSO-d_6) δ 169.0, 150.1, 149.4, 145.3, 139.8, 138.5, 136.7, 135.6, 132.7, 130.1, 129.8, 128.1, 122.5, 119.9, 118.4, 116.2, 62.3, 53.3, 49.0, 20.5, 19.5; HRMS (ESI): m/z $[M + H]^+$ calcd for $C_{25}H_{27}ClN_4O$: 435.1952; found: 435.1955.

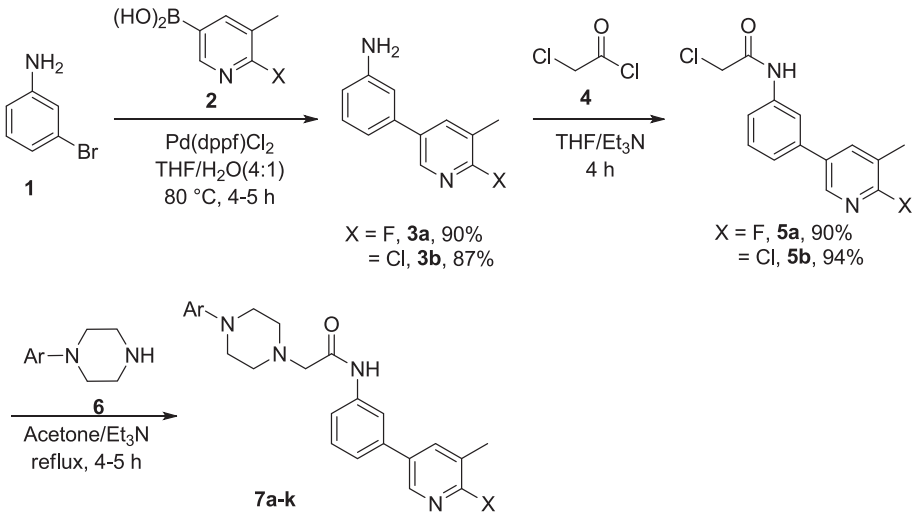

Scheme 1. Synthesis of piperazine tethered pyridine derivatives.

2.3.10. N-(3-(6-Chloro-5-methylpyridin-3-yl)phenyl)-2-(4-(4-chlorophenyl)piperazin-1-yl)acetamide (7j)

White solid; m.p. 146–148 °C; IR (neat): 3301, 2938, 1676, 1599, 1364, 976 cm^{-1}; ^1H NMR (400 MHz, DMSO-d_6) δ 9.93 (s, 1H, N—H), 8.55 (s, 1H, Ar—H), 8.10 (s, 1H, Ar—H), 8.01 (s, 1H, Ar—H), 7.82 (d, J = 8.0 Hz, 1H, Ar—H), 7.45–7.51 (m, 2H, Ar—H), 7.27 (d, J = 8.0 Hz, 2H, Ar—H), 7.00 (d, J = 8.0 Hz, 2H, Ar—H), 3.20–3.32 (m, 6H, CH_2 and m, 4H, $(CH_2)_2$), 2.67–2.78 (m, 4H, $(CH_2)_2$), 2.45 (s, 3H, CH_3); ^{13}C NMR (100 MHz, DMSO-d_6) δ 168.9, 150.3, 150.1, 145.3, 139.8, 138.5, 136.7, 135.6, 132.7, 130.1, 129.1, 122.8, 122.5, 119.9, 118.3, 117.3, 62.1, 53.0, 48.4, 19.5; HRMS (ESI): m/z $[M + H]^+$ calcd for $C_{24}H_{24}Cl_2N_4O$: 455.1405; found: 455.1408.

2.3.11. N-(3-(6-Chloro-5-methylpyridin-3-yl)phenyl)-2-(4-(2-fluorophenyl)piperazin-1-yl)acetamide (7 k)

Brown solid; m.p. 146–148 °C; IR (neat): 3303, 2940, 1674, 1596, 1368, 970 cm^{-1}; ^1H NMR (400 MHz, DMSO-d_6) δ 9.90 (s, 1H, N—H), 8.52 (s, 1H, Ar—H), 8.01–8.05 (m, 2H, Ar—H), 7.80 (d, J = 8.0 Hz, 1H, Ar—H), 7.41–7.48 (m, 2H, Ar—H), 6.98–7.15 (m, 4H, Ar—H), 3.25 (s, 2H, CH_2), 3.10–3.18 (m, 4H, $(CH_2)_2$), 2.65–2.80 (m, 4H, $(CH_2)_2$), 2.41 (s, 3H, CH_3); ^{13}C NMR (100 MHz, DMSO-d_6) δ 168.9, 161.3, 155.4 (d, J = 242.0 Hz), 150.1, 145.3, 140.3, 139.8, 138.4, 136.2 (d, J = 118.0 Hz), 132.6, 130.0, 125.2, 122.8, 122.4, 119.9, 119.7, 118.3, 116.4 (d, J = 20.0 Hz), 62.2, 53.3, 50.4, 19.5; HRMS (ESI): m/z $[M + H]^+$ calcd for $C_{24}H_{24}ClFN_4O$: 439.1701; found: 439.1703.

2.4. Molecular docking study

Molecular docking simulations were performed using Scripps Research Institute's AutoDock 4.2 Tools [21]. The three-dimensional structure of the BCL-XL protein in complex with a BAD peptide was provided by the RCSB Protein Data Bank (PDB ID: 1G5J). After all water molecules were removed from the protein structure, polar hydrogen atoms were added to ensure the appropriate protonation states for docking. The chemical structures of the compounds **7h** and NPB were constructed and geometrically optimized using suitable software. The resultant three-dimensional structures were saved in Mol2 format for AutoDock compatibility. After preparing the protein and ligand, AutoDock Tools (ADT) was used to set up the docking. Torsional degrees of freedom were established for the ligands and Kollman charges were assigned to the protein. A grid box was built around the hydrophobic groove of BCL-XL using the AutoGrid tool, with a grid spacing of 0.450 Å and grid size of 40 Å × 40 Å × 40 Å. The Lamarckian Genetic Algorithm (LGA) was used to run docking simulations. A maximum of 10 separate docking runs were performed on each compound, using the default docking settings. Predicted binding energy (kcal/mol) was used to rank the obtained binding conformations. BIOVIA Discovery Studio Visualizer [22] and UCSF Chimera [23] were used for post-docking analysis to assess hydrogen bonding patterns, binding poses and ligand-protein interactions.

Table 1
Yields and IC_{50} values of **7a-k.**

Entry	X	Ar	7	% Yield	IC_{50} ± SD against MCF-7 (μM)
1	F	2,3-$Cl_2C_6H_3$	7a	90	91.42 ± 1.52
2	F	4-ClC_6H_4	7b	88	59.89 ± 1.39
3	F	2-$NO_2C_6H_4$	7c	92	>100
4	F	2-F-4-Cl-C_6H_3	7d	91	>100
5	F	4-MeC_6H_4	7e	91	>100
6	F	2-FC_6H_4	7f	92	63.48 ± 1.12
7	Cl	2,3-$Cl_2C_6H_3$	7g	91	22.48 ± 0.65
8	Cl	2-$NO_2C_6H_4$	7h	94	6.15 ± 0.18
9	Cl	4-MeC_6H_4	7i	90	>100
10	Cl	4-ClC_6H_4	7j	90	30.13 ± 1.03
11	Cl	2-FC_6H_4	7k	89	16.99 ± 0.94

Note: Tamoxifen was used as a reference drug which showed IC_{50} of 1.75 ± 0.08 μM.

3. Results and discussion

3.1. Chemistry

We started synthesis (Scheme 1) by conducting the Suzuki coupling reaction between 3-bromoaniline **1** and (6-halo-5-methylpyridin-3-yl) boronic acid **2** in the presence of [1,1′-bis(diphenylphosphino)ferrocene]palladium(II) dichloride [Pd(dppf)Cl_2] in aqueous THF at 80 °C, which furnished 3-(6-fluoro/chloro-5-methylpyridin-3-yl)aniline **3** in 87–90 % yields. Later, acylation of **3** was conducted using chloroacetyl chloride **4** in THF in the presence of triethylamine, which afforded 2-chloro-*N*-(3-(6-fluoro/chloro-5-methylpyridin-3-yl)phenyl)acetamide **5** in 90–94 % yields. Finally, various 1-arylpiperazines **6** was alkylated using 5, to get piperazine tethered pyridine derivatives **7a-k** in 88–94 % yields. The various substitutions used and the yields of corresponding products are presented in Table 1. All title compounds were characterized by IR, NMR and HRMS.

3.2. Biology

We tested all title compounds **7a-k** for their cytotoxicity against

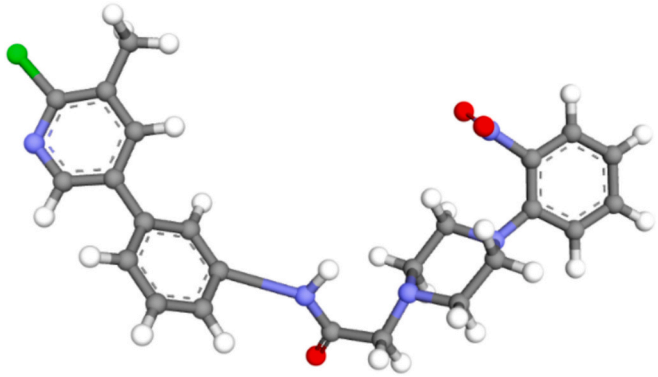

Fig. 2. 3D-structure of compound **7 h.**

MCF-7 human breast cancer cell lines and their IC_{50} values are given in Table 1. It appears that chlorine (X = Cl) on pyridine is more effective than fluorine (X = F) as evident from the data that in the former case IC_{50} values ranges from 6.15 to 30.13 μM and in the latter case IC_{50} values span between 59.89 and 91.42 μM. Further, three compounds are ineffective when X is fluoro and a compound is less effective when X is chloro. Keeping fluorine on pyridine as a constant substituent and structural variations on aryl ring attached piperazine indicated that chlorine is a better substituent at *p*-position (59.89 μM) than methyl at *p*-position (>100 μM). Introduction of chloro groups at *o*- and *m*-position (on Ar) reduced the activity to 91.42 μM. Fluorine (on Ar) at *o*-position (63.48 μM) is better than nitro (>100 μM). On the other hand, when chlorine on pyridine is a constant substituent, methyl group (on Ar) at *p*-position is ineffective and other substituents like chloro, nitro and fluoro enhanced the activity. Among, nitro at *o*-position (6.15 μM) is the best substituent. Its replacement by fluorine reduced the activity to 16.99 μM. Regrettably, all compounds are poorer than reference drug Tamoxifen which showed IC_{50} of 1.75 μM against MCF-7.

3.3. Molecular docking study

In order to perform the docking simulation, the three-dimensional structure of the compound **7h** was prepared and energy-optimized using the Avogadro software (Fig. 2) [24]. As shown in the Fig. 3a cartoon representation of the BAD peptide(yellow) in complex with BCL-XL protein (green) was taken as the target for molecular docking studies. Compound **7h** was put through molecular docking analysis in order to clarify the exact molecular interactions and analyse the binding affinity between small molecule and active site residues of the target protein complex of BCL-XL with peptide from BAD (PDB ID: 1G5J). A very stable binding model was found by docking simulations, indicating a strong interaction between compound **7h** and the hydrophobic groove of pro-survival protein BCL-XL (Fig. 4). The compound was found to be binding to the hydrophobic groove of BCL-XL where the BAD was bound (Fig. 3b). The predicted binding energy for the compound **7h** was −7.74 kcal/mol. To further analyse the docking efficiency of this compound, it was compared with NPB,[10] which also had the similar binding pattern (Fig. 3c). According to these studies, the compound interacted by forming conventional hydrogen bonds with SER-110, GLN-115 along with carbon hydrogen bonds with SER-126 and VAL-130. Amide-Pi-Stacked and Pi-Pi T-shaped bond with PHE-150 and GLN-129. Stability of a ligand-receptor complex was also enhanced by Pi-Sigma bond with ALA-108. Multiple stabilizing hydrophobic interactions were also noted, which showed the structural fit of **7h** within the hydrophobic groove of the targeted BCL-XL protein. These interactions enhanced van der Waals bond and suggested a good steric fit of the ligand within the BCL-XL binding pocket (Fig. 5).

4. Conclusion

In summary, we have synthesized a series of piperazine tethered pyridine derivatives in three simple steps. We evaluated these compounds for their cytotoxic activities against MCF-7 breast cancer cell lines. Among the tested compounds, *N*-(3-(6-chloro-5-methylpyridin-3-yl)phenyl)-2-(4-(2-nitrophenyl)piperazin-1-yl)acetamide **7 h** has emerged as a lead candidate with IC_{50} value 6.15 μM. The structure activity relationship analysis showed that chloro on pyridine moiety is better than fluoro. Further, nitro group at *o*-position of aryl ring attached to piperazine moiety is better than chloro, fluoro and methyl groups. The possible mode of action of these molecules has been predicted with the molecular modeling. Thus, it showed that our molecules induced apoptosis by inhibiting phophorylation of BAD. Even though our lead molecule has showed cytotoxity lesser than reference drug Tamoxifen (1.75 μM), it is still a better drug candidate since it has not affected healthy HEK cells at its cytotoxic concentration (6.15 μM). The future study demands further modification of the lead molecule for better

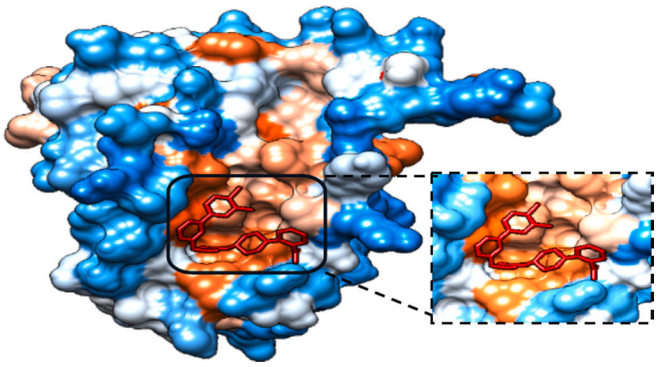

Fig. 4. 3D Surface view of **7h** binding to the hydrophobic groove of BCL-XL (hydrophobic amino acids are shown in red). (For interpretation of the references to colour in this figure legend, the reader is referred to the web version of this article.)

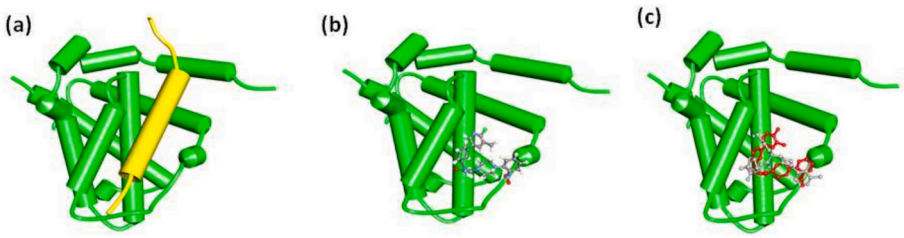

Fig. 3. Docking studies of **7h** with respect to the BCL-XL/BAD interface. **(a)** The Protein Data Bank ID 1G5J was utilized to model the complex of BCL-XL (green cartoon) with a 25-residue helical segment of BAD (yellow cartoon). **(b)** Structure of the small molecule **7h** as determined by NMR in stick representation binding to a groove within the BCL-XL protein–protein interface. **(c)** Predicted **7h** binding mode to BCL-XL: **7h** binds at a region comparable to that of an NPB. (For interpretation of the references to colour in this figure legend, the reader is referred to the web version of this article.)

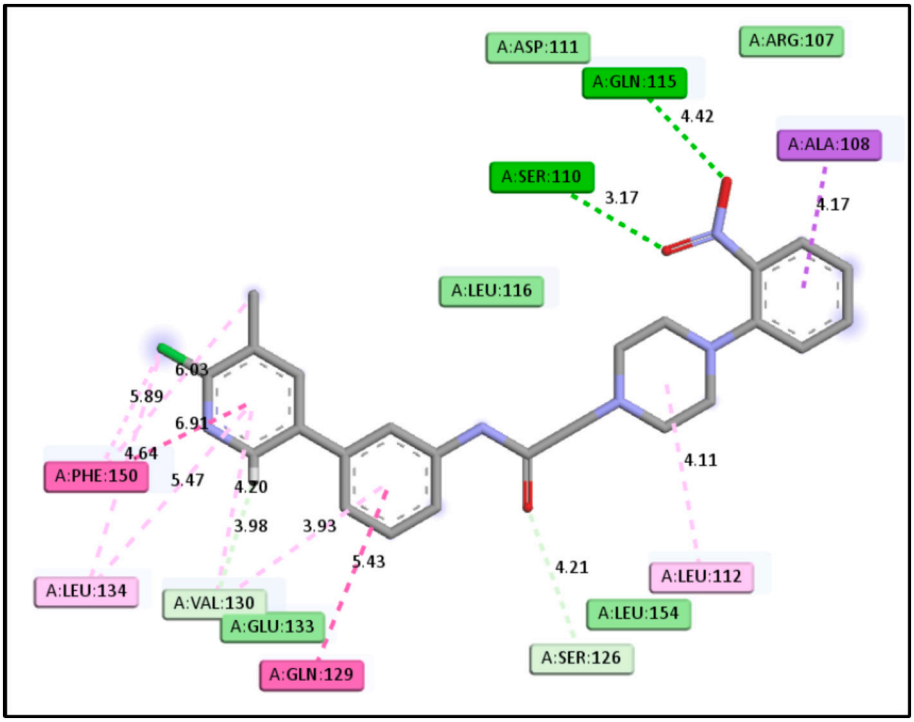

Fig. 5. Two-dimensional illustration of **7h** interaction with the hydrophobic groove residues, which are necessary for binding.

activity. Further, development of novel anticancer agents is in progress in our laboratory.

CRediT authorship contribution statement

Dileep Nagaraju: Methodology. **Pushpa H. Chandraiah:** Funding acquisition. **Bhoomika B. Ravi:** Software, Data curation. **Sindhu M. Parameshwaraiah:** Conceptualization. **Mamatha S. Kempasiddegowda:** Data curation. **Toreshettahally R. Swaroop:** Writing – original draft, Validation. **Santosh L. Goankar:** Resources. **Kanchugarakoppal S. Rangappa:** Supervision. **Basappa Basappa:** Writing – review & editing, Supervision.

Declaration of competing interest

The authors declare that they have no known competing financial interests or personal relationships that could have appeared to influence the work reported in this paper.

Acknowledgments

DN thanks CSIR for JRF. BBR thanks University of Mysore for OBC fellowship. BB acknowledge VGST project. KSR thanks NASI for distinguished chair professor. All authors thank Prof. Peter E Lobie for biological studies.

Appendix A. Supplementary data

Supplementary data to this article can be found online at https://doi.org/10.1016/j.rechem.2025.102907.

Data availability

Data will be made available on request.

References

[1] M. Faizan, R. Kumar, A. Mazumder, Kukreti N. Salahuddin, A. Kumar, M.V.N. L. Chaitanya, The medicinal chemistry of piperazines: a review, Chem. Biol. Drug Des. 103 (2024) e14537, https://doi.org/10.1111/cbdd.14537.
[2] S. Singh, R. Kumar, S. Tripathi, Mazumder A. Salahuddin, N. Singh, Fused and substituted piperazines as anticancer agents: a review, Chem. Biol. Drug Des. 105 (2025) e70077, https://doi.org/10.1111/cbdd.70077.
[3] D. Sahu, P.S.R. Sreekanth, P.K. Behera, M.K. Pradhan, A. Patnaik, S. Salunkhe, R. Cep, Advances in synthesis, medicinal properties and biomedical applications of pyridine derivatives: a comprehensive review, Eur. J. Med. Chem. Rep. 12 (2024) 100210, https://doi.org/10.1016/j.ejmcr.2024.100210.
[4] S. De, S.K.A. Kumar, S.K. Shah, S. Kazi, N. Sarkar, S. Banerjee, S. Dey, Pyridine: the scaffolds with significant clinical diversity, RSC Adv. 12 (2022) 15385–15406, https://doi.org/10.1039/D2RA01571D.
[5] E.A. Mohamed, N.S.M. Ismail, M. Hagras, H. Refaat, Medicinal attributes of pyridine scaffold as anticancer targeting agents, Futur J. Pharm. Sci. 7 (2021) 24, https://doi.org/10.1186/s43094-020-00165-4.
[6] J. Zha, H. Harada, K. Osipov, J. Jockel, G. Waksman, S.J. Korsmeyer, BH3 domain of BAD is required for heterodimerization with BCL-XL and pro-apoptotic activity, J. Biol. Chem. 272 (1997) 24101–24104, https://doi.org/10.1074/jbc.272.39.24101.
[7] Y. Wang, Y.S. Chiou, Q.Y. Chong, M. Zhang, K.S. Rangappa, M. Ma, et al., Pharmacological inhibition of BAD Ser99 phosphorylation enhances the efficacy of cisplatin in ovarian cancer by inhibition of cancer stem cell-like behavior, ACS Pharm. Transl. Sci. 3 (2020) 1083–1099, https://doi.org/10.1021/acsptsci.0c00064.
[8] S.R. Datta, A. Brunet, M.E. Greenberg, Cellular survival: a play in three Akts, Genes Dev. 13 (1999) 2905–2927, https://doi.org/10.1101/gad.13.22.2905.
[9] N.L. Bui, V. Pandey, T. Zhu, L. Ma, Lobie P.E. Basappa, Bad phosphorylation as a target of inhibition in oncology, Cancer Lett. 415 (2018) 177–186, https://doi.org/10.1016/j.canlet.2017.11.017.
[10] V. Pandey, B. Wang, C.D. Mohan, A.R. Raquib, S. Rangappa, V. Srinivasa, et al., Discovery of a small-molecule inhibitor of specific serine residue BAD phosphorylation, Proc. Natl. Acad. Sci. USA 115 (2018) E10505–E10514, https://doi.org/10.1073/pnas.1804897115.
[11] P.E. Lobie, V.K. Pandey, K.S. Rangappa, Mohan C.D. Basappa, S. Rangappa, et al., World intellectual property organization, WO2018194520 A1 (2018).
[12] N. Rajeev, T.R. Swaroop, S.M. Anil, K.R. Kiran, K.S. Rangappa, M.P. Sadashiva, A sequential one-pot tandem approach for the synthesis of 4-tosyl-5-aryloxazoles from carboxylic acids, J. Chem. Sci. 30 (2018) 150, https://doi.org/10.1007/s12039-018-1540-2.
[13] C. Santhosh, K. Ravi Singh, K. Sheela, T.R. Swaroop, M.P. Sadashiva, Regioselective synthesis of 2,5-disubstituted-1,3,4-thiadiazoles and 1,3,4-oxadiazoles *via* alkyl 2-(methylthio)-2-thioxoacetates and alkyl 2-amino-2-thioxoacetates, J. Org. Chem. 88 (2023) 11486–11496, https://doi.org/10.1021/acs.joc.3c00589.

[14] T.R. Swaroop, Z.-Q. Wang, Q.Y. Li, H.-S. Wang, Reductive coupling of aromatic aldehydes and ketones under electrochemical conditions, J. Electrochem. Soc. 167 (2020) 046504, https://doi.org/10.1149/1945-7111/ab72ed.
[15] R. Roopashree, C.D. Mohan, T.R. Swaroop, S. Jagadish, K.S. Rangappa, Synthesis, characterization and in vivo biological evaluation of novel benzimidazoles as potential anticancer agents, Asian J. Pharm. Clin. Res. 7 (2014) 309–313, https://journals.innovareacademics.in/index.php/ajpcr/article/view/1875.
[16] S.D. Preethi, K.S. Balaji, D.S. Prasanna, T.R. Swaroop, J. Shankar, K.S. Rangappa, et al., Synthesis, characterization of 4-anilino-6,7-dimethoxy quinazoline derivatives as potential anti-angiogenic agents, Anti Cancer Agents Med. Chem. 17 (2017) 1931–1941, https://doi.org/10.2174/1871521409666170412120837.
[17] H. Swetha, T.R. Swaroop, H.D. Preetham, C.D. Mohan, M. Umashakara, Basappa, et al., Synthesis, cytotoxic and heparanase inhibition studies of 5-oxo-1-arylpyrrolidine-3-carboxamides of hydrazides and 4-amino-5-aryl-4*H*-1,2,4-triazole-3-thiol, Curr. Org. Synth. 17 (2020) 243–250, https://doi.org/10.2174/1570179417666200225123329.
[18] H.M. Poh, Y.S. Chiou, Q.Y. Chong, R.M. Chen, K.S. Rangappa, L. Ma, et al., Inhibition of TFF3 enhances sensitivity—and overcomes acquired resistance—to doxorubicin in estrogen receptor-positive mammary carcinoma, Cancers 11 (2019) 1528, https://doi.org/10.3390/cancers11101528.
[19] M. Gilandoust, K.B. Harsha, C.D. Mohan, A.R. Raquib, S. Rangappa, V. Pandey, et al., Synthesis, characterization and cytotoxicity studies of 1,2,3-triazoles and 1,2,4-triazolo [1,5-*a*] pyrimidines in human breast cancer cells, Bioorg. Med. Chem. Lett. 28 (2018) 2314–2319, https://doi.org/10.1016/j.bmcl.2018.05.020.
[20] Q.Y. Chong, M.L. You, V. Pandey, A. Banerjee, Y.J. Chen, H.M. Poh, et al., Release of HER2 repression of trefoil factor 3 (TFF3) expression mediates trastuzumab resistance in HER^{2+}/ER^{+} mammary carcinoma, Oncotarget 8 (2017) 74188–74208, https://doi.org/10.18632/oncotarget.18431.
[21] D.S. Goodsell, M.F. Sanner, A.J. Olson, S. Forli, The AutoDock suite at 30, Protein Sci. 30 (2021) 31–43, https://doi.org/10.1002/pro.3934.
[22] BIOVIA Dassault Systèmes, Discovery Studio Visualizer, 21.1.0.20298; Dassault Systèmes: San Diego, CA, USA, 2020.
[23] E.F. Pettersen, T.D. Goddard, C.C. Huang, G.S. Couch, D.M. Greenblatt, E.C. Meng, et al., UCSF Chimera–a visualization system for exploratory research and analysis, J. Comput. Chem. 25 (2004) 1605–1612, https://doi.org/10.1002/jcc.20084.
[24] M.D. Hanwell, D.E. Curtis, D.C. Lonie, T. Vandermeersch, E. Zurek, G.R. Hutchison, Avogadro: an advanced semantic chemical editor, visualization, and analysis platform, J. Chemother. 4 (2012) 17, https://doi.org/10.1186/1758-2946-4-17.